Probing Quantum Thermalization of a Disordered Dipolar Spin Ensemble with Discrete Time-Crystalline Order

Joonhee Choi,[1,2,*] Hengyun Zhou,[1,*] Soonwon Choi,[1] Renate Landig,[1] Wen Wei Ho,[1] Junichi Isoya,[3] Fedor Jelezko,[4] Shinobu Onoda,[5] Hitoshi Sumiya,[6] Dmitry A. Abanin,[7] and Mikhail D. Lukin[1,†]

[1]*Department of Physics, Harvard University, Cambridge, Massachusetts 02138, USA*
[2]*School of Engineering and Applied Sciences, Harvard University, Cambridge, Massachusetts 02138, USA*
[3]*Faculty of Pure and Applied Sciences, University of Tsukuba, Tsukuba, Ibaraki 305-8573 Japan*
[4]*Institut für Quantenoptik, Universität Ulm, 89081 Ulm, Germany*
[5]*Takasaki Advanced Radiation Research Institute, National Institutes for Quantum and Radiological Science and Technology, 1233 Watanuki, Takasaki, Gunma 370-1292, Japan*
[6]*Sumitomo Electric Industries Ltd., Itami, Hyougo, 664-0016, Japan*
[7]*Department of Theoretical Physics, University of Geneva, 1211 Geneva, Switzerland*

(Received 26 June 2018; revised manuscript received 19 November 2018; published 1 February 2019)

We investigate thermalization dynamics of a driven dipolar many-body quantum system through the stability of discrete time crystalline order. Using periodic driving of electronic spin impurities in diamond, we realize different types of interactions between spins and demonstrate experimentally that the interplay of disorder, driving, and interactions leads to several qualitatively distinct regimes of thermalization. For short driving periods, the observed dynamics are well described by an effective Hamiltonian which sensitively depends on interaction details. For long driving periods, the system becomes susceptible to energy exchange with the driving field and eventually enters a universal thermalizing regime, where the dynamics can be described by interaction-induced dephasing of individual spins. Our analysis reveals important differences between thermalization of long-range Ising and other dipolar spin models.

DOI: 10.1103/PhysRevLett.122.043603

Thermalization is a universal feature of most many-body systems [1–8], underlying the applicability of equilibrium statistical mechanics. At the same time, it represents an important limitation for the coherent manipulation of large scale quantum systems in quantum information processing. For these reasons, a detailed understanding of thermalization processes in closed, interacting quantum many-body systems is of great interest to both fundamental and applied science.

Over the last few decades, it has been demonstrated both theoretically and experimentally that thermalization processes in many-body systems can be significantly slowed, or even halted due to strong disorder [9–19]. The suppression of thermalization allows for novel nonequilibrium states of matter that would otherwise be forbidden in equilibrium. One remarkable example is the discrete time crystal phase in periodically driven (Floquet) systems [20–25]. This phase is characterized by a spontaneous breaking of the discrete time-translational symmetry of the drive, which is manifested in local observables exhibiting long-lived, robust oscillations at a subharmonic of the fundamental driving frequency. Signatures of discrete time-crystalline (DTC) order have been observed in various experimental platforms such as trapped ions, electronic and nuclear spin ensembles [26–29]. Since the stability of DTC order is closely related to the suppression of thermalization processes, these observations also raise the intriguing possibility of using the DTC signal as a tool to study thermalization dynamics in an interacting many-body system.

In this Letter, we demonstrate that the stability of DTC order can be used as a sensitive, quantitative probe of thermalization behavior in a quantum many-body dipolar system. Specifically, we coherently manipulate a disordered ensemble of dipolar-interacting spins to engineer Floquet dynamics with three different types of interactions. In all cases, robust, long-lived signatures of DTC order can be observed over some range of parameters. By tuning both the Floquet period and the strength of perturbations, we monitor the corresponding changes in the decay of DTC order that ensue, which allows us to study thermalization dynamics in these systems.

Our experimental observations reveal the presence of three distinct thermalization regimes. In the case where the driving period is short compared to the inverse of disorder strength, DTC order is robust over a wide range of perturbation strengths, and we find that spin dynamics is well described by a time-averaged Hamiltonian which sensitively depends on the details of interactions [24,30–33]. Thermalization occurs only via rare resonances that are strongly suppressed by the large disorder [34–36]. At longer periods, the average Hamiltonian description breaks

down as the system can exchange energy with the periodic drive, but long-lived DTC order can still persist. This stability can be attributed to critically slow thermalization dynamics arising from the delicate interplay of the long-range nature of interactions with disorder and driving, in agreement with previous observations of a critical DTC regime [17,25,27]. At sufficiently long drive periods, DTC order becomes unstable as the system enters a third thermalizing regime, characterized by universal dynamics independent of the interaction details. The universal behavior is consistent with Markovian dephasing of individual spins, implying that the many-body system serves as its own Markovian bath [4,6,37–39]. However, we find that the crossover to this regime depends strongly on the nature of interactions, indicating differences in thermalization dynamics of long-range Ising and other dipolar spin models [40]. Our results have important implications for the dynamical engineering of Hamiltonians [41,42], novel Floquet phases in many-body systems [43–48], with applications to quantum metrology [49] and quantum simulations [50].

Experimental setup.—Our experiments employ a dense ensemble of nitrogen-vacancy (NV) centers in diamond [51]. Each NV center comprises an $S = 1$ electronic spin with internal states $|m_s = 0, \pm 1\rangle$, which can be initialized, manipulated, and read out by optical and microwave pulses. The high NV center concentration (∼45 ppm) in our sample provides strong magnetic dipolar interactions between spins, with interaction strengths significantly exceeding extrinsic decoherence rates [17,52]. Our sample has also various sources of disorder, with an energy scale generally larger than the interaction strength between NV centers. A more detailed characterization can be found in Refs. [17,52,53].

To probe thermalization dynamics, we use pulsed periodic microwave driving to engineer three distinct types of Floquet evolutions, which we denote as $\mathbb{Z}_2$ Ising, $\mathbb{Z}_2$, $\mathbb{Z}_3$. In all cases, a Floquet cycle consists of time evolution under an interacting Hamiltonian for a tunable duration τ_1, followed by strong microwave pulses effecting a global spin rotation:

$$U_F^{(a)} = P_\theta^{(a)} \exp[-iH^{(a)}\tau_1], \tag{1}$$

where $a \in \{\mathbb{Z}_2\text{-Ising}, \mathbb{Z}_2, \mathbb{Z}_3\}$, $P_\theta^{(a)}$ is the spin rotation parametrized by a tunable angle θ, and $H^{(a)}$ is an effective Hamiltonian for relevant degrees of freedom of the spin ensemble, containing interaction and disorder terms [Fig. 1(a)]. The time durations of $P_\theta^{(a)}$ are fixed at $\tau_2 =$ 10 ns ($\mathbb{Z}_2$ Ising and $\mathbb{Z}_2$) or $\tau_2 = 20$ ns ($\mathbb{Z}_3$), such that the Floquet time period $T = \tau_1 + \tau_2$ is dominated by τ_1. For $\mathbb{Z}_2$ Ising and $\mathbb{Z}_2$, the microwave excitation $P_\theta^{(a)}$ is resonant with the $|0\rangle \leftrightarrow |-1\rangle$ transition, and these two states form an effective two-level system. For $\mathbb{Z}_3$, $P_\theta^{\mathbb{Z}_3}$ consists of two

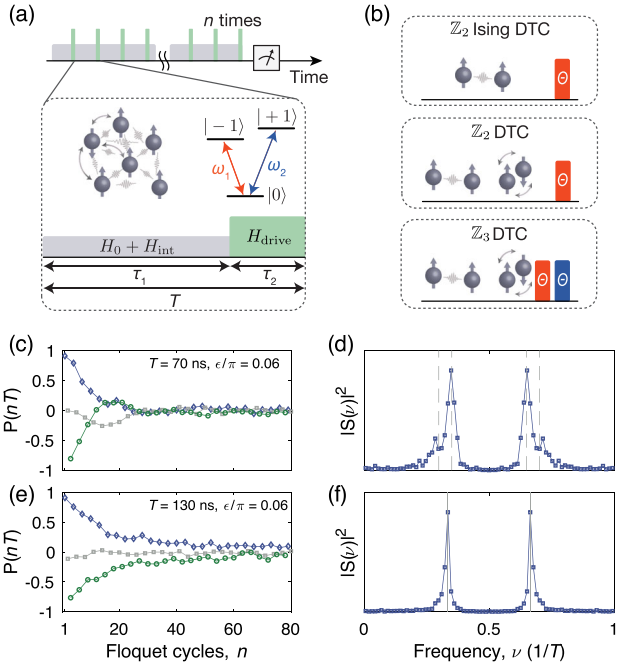

FIG. 1. Experimental system and observation of DTC order. (a) Periodically driven, interacting NV centers. During each Floquet period T (dotted box), NV centers interact for time τ_1, then experience pulsed microwave rotations of duration τ_2, at resonant frequencies ω_1 or ω_2. After n Floquet cycles, the population difference between $|0\rangle$ and $|-1\rangle$ is measured. (b) Distinct Floquet time evolutions realized: $\mathbb{Z}_2$ Ising, with only Ising interactions, and $\mathbb{Z}_2$ and $\mathbb{Z}_3$, with both Ising and spin-exchange interactions. (c)–(f) Representative time traces of the normalized spin polarization $P(nT)$ and Fourier spectra $|S(\nu)|^2$ of the $\mathbb{Z}_3$ DTC order at a perturbation $\epsilon/\pi = 0.06$ with $T = 70$ ns (c), (d) and 130 ns (e),(f). In (c),(e), blue, gray, and green points correspond to $P(t)$ at $t \equiv T, 2T, 3T$ (mod $3T$), respectively.

consecutive pulses, resonant with $|0\rangle \leftrightarrow |\pm 1\rangle$ transitions, thereby exploiting all three spin states [Fig. 1(b)]. In the ideal case $\theta = \pi$, $P_\pi^{(a)}$ permutes the populations between two (three) spin states such that they return to the original configuration after two (three) cycles. In the following experiments, we introduce systematic perturbations $\epsilon = \theta - \pi$, whose accuracy is limited to about 1% due to spatial inhomogeneity of the applied field and disorder in the system [52].

The effective spin-spin interactions are different in the three cases. For $\mathbb{Z}_2$ and $\mathbb{Z}_3$, spins interact via natural dipole-dipole interactions, which involve both Ising-type interactions and spin exchange between resonant transitions, e.g., $|0\rangle_i \otimes |\pm 1\rangle_j \leftrightarrow |\pm 1\rangle_i \otimes |0\rangle_j$ for spins i, j [52]. For $\mathbb{Z}_2$ Ising, strong transverse microwave driving during τ_1 causes the spin-spin interactions in the dressed state basis $|\pm X\rangle = (|0\rangle \pm |-1\rangle)/\sqrt{2}$ to become purely Ising-like [52]. In our experiments, spins are initially polarized along the corresponding quantization axes ($|0\rangle$ for $\mathbb{Z}_2$, $\mathbb{Z}_3$ and $|+X\rangle$ for $\mathbb{Z}_2$ Ising). After time evolution by the Floquet

unitary $U_F^{(a)}$ for n cycles, the remaining polarization $P(nT)$ along the initialization axis is measured via spin-state-dependent fluorescence.

Experimental observations and analyses.—In all three cases, we observe robust subharmonic responses over a wide range of perturbation strengths ϵ and Floquet periods T. As an example, Figs. 1(c)–1(f) shows typical time traces of $P(nT)$ and their Fourier spectra $|S(\nu)|^2$ for $\mathbb{Z}_3$, for two different T at finite ϵ [52]. For very short T, $P(nT)$ shows a modulated decaying signal, and $|S(\nu)|^2$ displays broad side peaks at ϵ-dependent locations away from $\nu = 1/3$ [Figs. 1(c), 1(d)]. For larger T, $P(nT)$ instead exhibits long-lived oscillations with a period of three cycles, reflected in a sharp spectral peak pinned at $\nu = 1/3$, indicating that the subharmonic response is stabilized by interactions [Figs. 1(e), 1(f)]. Generally, for an integer $m > 1$, we associate the signature of $\mathbb{Z}_m$ DTC order with the presence of $\nu = 1/m$ peaks in the Fourier spectrum that are sharp and robust against perturbations ϵ.

To quantitatively probe the stability of DTC order as a function of parameters ϵ and T, we examine the crystalline fraction f, defined as the normalized spectral weight at the expected frequency $\nu = 1/m$ $(m = 2, 3)$ in the late time $(n \geq 40)$ dynamics of $P(nT)$, after initial transients in the dynamics have decayed away. For each T, we identify the value of ϵ at $f = 0.1$ as the phenomenological phase boundary where DTC order is lost [Figs. 2(a)–2(c)]. Focusing first on short T, we find in all three cases that the phase boundaries are linear in the $\epsilon - T$ plane, similar to prior observations [26–28]. However, closer inspection [Fig. 2(d)] reveals that DTC order extends to a wider range of ϵ in $\mathbb{Z}_2$ & $\mathbb{Z}_3$ than in $\mathbb{Z}_2$ Ising. This is surprising since spin-exchange interactions should intuitively aid thermalization and make DTC order less stable, although it is known that long-range interactions can sometimes have a regularizing effect on dynamics [54].

From Figs. 2(a)–2(c), we observe that the linear phase boundaries do not extend indefinitely with increasing T, but instead bend inwards, albeit with different shapes between the different Floquet Hamiltonians. To investigate thermalization dynamics in this longer T regime, we examine the decay of DTC order. Specifically, we perform a Fourier transform of $P(nT)$ over a window of cycles $n \in [n_{\text{sweep}}, n_{\text{sweep}} + L - 1]$, where $L = 36$ is fixed, and extract the subharmonic peak height $\mathcal{S} = |S(\nu = 1/m)|^2$, $(m = 2, 3)$. By sweeping the starting position n_{sweep}, we produce a time trace of the peak height, which allows us to track how the DTC order decays in time. Figures 3(a)–3(b) shows typical decay profiles of $\mathbb{Z}_3$ DTC order, for two different T. For T slightly beyond the linear phase boundary regime, the decay exhibits a stretched exponential profile, with late-time decay rates Γ nearly independent of ϵ [Fig. 3(a)]. In contrast, for long T, the decay profile of $\mathcal{S}$ approaches a simple exponential, characteristic of Markovian dynamics [Fig. 3(b)]. Γ also becomes sensitive to ϵ, indicating an instability of the subharmonic signal [Fig. 3(c)]. We have verified that the other Floquet Hamiltonians also exhibit qualitatively similar changes in the behavior of $\mathcal{S}$ [52].

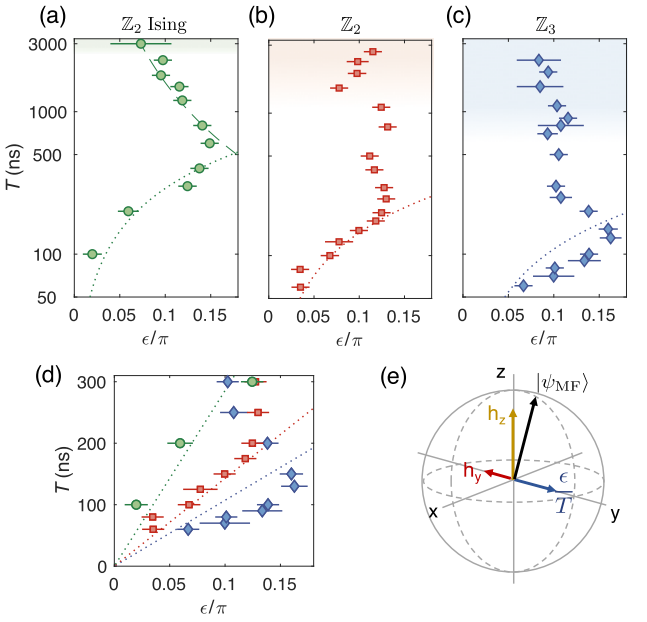

FIG. 2. Phase diagram of DTC order for short drive periods. (a)–(c) Phase diagrams in semi-log scale. The phase boundary (markers) is identified as a crystalline fraction of 10%. The dotted line indicates the linear phase boundary predicted by a self-consistent mean-field analysis [52]. Shaded areas denote a universal dephasing regime corresponding to Markovian thermalization where $T > T^*$ (see Fig. 4). In (a), the dashed line represents the theoretical prediction from Ref. [25]. Errorbars denote 95% confidence intervals of the phase boundary [52]. (d) Short-T phase diagram in linear scale [markers as in (a)–(c)]. (e) Bloch sphere illustrating the screening effect of spin-exchange interactions. h_z and h_y are mean fields arising from Ising and spin-exchange interactions, respectively, and ϵ/T is the perturbing field. The black arrow corresponds to the mean field solution $|\psi_{\text{MF}}\rangle$.

To quantify the crossover between different decay profiles, we phenomenologically fit $\mathcal{S}$ with a stretched exponential $A \exp[-(n_{\text{sweep}}/n_T)^{\beta}]$. For a given T, we compute the exponent $\bar{\beta}$ governing the decay of the stretched exponential, averaged over different ϵ. For all Floquet sequences, we find that $\bar{\beta}$ increases from ~0.6 (stretched exponential) with increasing T, before saturating at 1 (single exponential), albeit with different saturation timescales T^* [Fig. 4(a)]. We note there is a slight falling off for very long T, which we attribute to convolution effects with the longitudinal spin relaxation (T_1) [52,53]. We employ a saturation fit $\bar{\beta} = 1/[1 + (c_1/T)^{c_2}]$ and extract the Floquet period T^* at which $\bar{\beta} = 0.9$. Interestingly, T^* coincides with the timescale beyond which Γ as a function of ϵ collapses onto a universal quadratic shape, with curvature approximately equal to $1/2$ up to an offset Γ_0 [Fig. 4(b)].

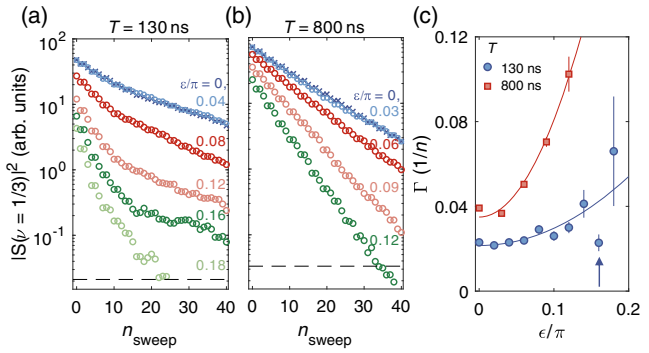

FIG. 3. Long interaction time behavior of DTC order. (a), (b) Temporal decay of $\mathbb{Z}_3$ DTC order $|S(\nu = 1/3)|^2$, for different ϵ, as a function of sweeping window position n_{sweep}. Dashed lines denote the noise floor. (c) Late-time decay rate Γ as a function of ϵ, with phenomenological quadratic fit. Each data point results from an average over simple exponential fits of $|S(\nu = 1/3)|^2$ starting from $n_{\mathrm{sweep}} = 15$–20 to exclude initial transients resulting from a short-time, non-universal dephasing. Error bars denote the statistical error of the fit results. The arrow indicates the mean-field phase boundary.

Physically, Γ_0 is attributable to a combination of T_1 depolarization of spins and dephasing during the finite rotation pulses [52]. For the $\mathbb{Z}_2$-Ising, $\mathbb{Z}_2$, and $\mathbb{Z}_3$ cases, we find that $T^* = 2.64(5)$, $1.20(5)$, and $0.45(2)$ μs, respectively. As expected, T^* is longest for the $\mathbb{Z}_2$-Ising case, indicating that thermalization proceeds slower when only Ising interactions are present.

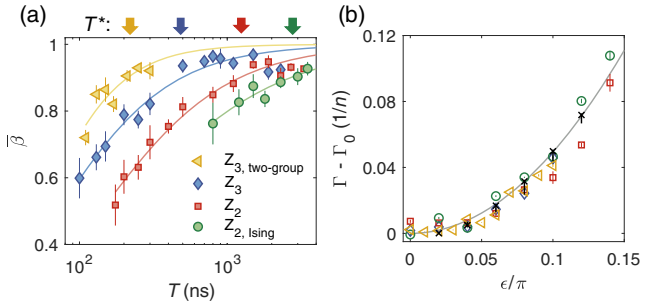

FIG. 4. Universal thermalization dynamics for different Floquet Hamiltonians. (a) Exponents of the stretched exponential fits versus T. Data points denote the average over β values extracted at different ϵ, error bars are the standard deviation of the mean. Lines denote fits to extract the saturation timescale T^* (arrows), identified where $\bar{\beta} = 0.9$. (b) Late-time decay rate Γ as a function of ϵ (after a global offset Γ_0 has been subtracted, see [52]) at $T = 3.5$, 3.5, 2.3, and 0.3 μs for the $\mathbb{Z}_2$-Ising, $\mathbb{Z}_2$, $\mathbb{Z}_3$, and two-group $\mathbb{Z}_3$ cases, respectively [markers as in (a)]. Solid line indicates a dephasing model fit, predicting $\Gamma = \epsilon^2/2 + \Gamma_0$. Error bars as in Fig. 3(c). Cross markers show numerical results of an infinite-range, interacting spin system with both Ising and spin-exchange interactions [52]. Error bars in the numerics represent the standard deviation of decay rate distributions for different realizations.

Discussion.—The above observations suggest the existence of three thermalization regimes: a short-T regime where spin-exchange interactions seem to stabilize DTC order, an intermediate-T regime where DTC order persists but is less stable, and a long-T, apparently universal regime where subharmonic responses are unstable, decaying at a rate $\Gamma = \epsilon^2/2$, and thus cannot be associated with stable DTC order.

To explain our observations in the short-T regime, we turn to a mean-field analysis. When T is sufficiently short compared to the inverse of disorder strength, we can describe the dynamics of the amplitude of $P(nT)$ by an effective, static Hamiltonian D by going into an appropriately chosen moving frame (the so-called toggling frame [52]). Keeping only the lowest order terms in T and ϵ, we obtain

$$D^{\mathbb{Z}_2\mathrm{Ising}} = \sum_{ij} \frac{J_{ij}}{r_{ij}^3} S_i^x S_j^x + \frac{\epsilon}{T} \sum_i S_i^y,$$

$$D^{\mathbb{Z}_2} = \sum_{ij} \frac{J_{ij}}{r_{ij}^3} (S_i^x S_j^x + S_i^y S_j^y - S_i^z S_j^z) + \frac{\epsilon}{T} \sum_i S_i^y,$$

$$D^{\mathbb{Z}_3} = \sum_{ij} \frac{J_{ij}}{r_{ij}^3} \sum_{ab} \left(\delta_{ab} - \frac{1}{3} \delta_{a\pm 1,b} \right) \sigma_i^{ab} \sigma_j^{ba} + \frac{\epsilon}{3T} \sum_i R_i,$$

where J_{ij}, r_{ij} are the orientation-dependent coefficient of dipolar interactions and distance between spins i, j, S_i^μ, are spin-1/2 operators for the two levels $|0\rangle$, $|-1\rangle$, $R_i = (\sigma_i^{+1,0} + \sigma_i^{-1,0} + i\sigma_i^{+1,-1} + \mathrm{H.c.})$, and $\sigma_i^{ab} = |a\rangle\langle b|$ with a, $b \in \{0, \pm 1\}$. Now, for each Hamiltonian, we seek a self-consistent steady-state solution at the mean-field level in the toggling frame, corresponding to a stable subharmonic response in the lab frame. We find that such solutions exist when $|\epsilon| \leq \epsilon_c = a J_{\mathrm{MF}} T$, where J_{MF} is the total mean-field interaction strength and a equals $1/2$, 1, and $4/3$ for $\mathbb{Z}_2$ Ising, $\mathbb{Z}_2$, and $\mathbb{Z}_3$ DTC, respectively, which yields a linear phase boundary prediction in reasonable agreement with the experimental data [Fig. 2(d)]. The wider phase boundary in $\mathbb{Z}_2$, $\mathbb{Z}_3$ than $\mathbb{Z}_2$ Ising can also be understood from the self-consistent mean-field wave function: one finds that spin-exchange terms, having opposite signs to the Ising terms, generate a screening field that partially cancels the perturbing external field [see Fig. 2(e), [52]].

The preceding mean-field analysis is expected to break down when T is larger than the inverse of disorder energy scales. Then, resonances due to absorption or emission of energy quanta from (into) the drive can occur more readily, giving rise to more thermalization channels. However, the apparent stability of the DTC order even in this regime can be explained—at least in the $\mathbb{Z}_2$-Ising case—by a critical DTC regime [25], in which the interplay of long-range interactions, dimensionality, disorder, and driving leads to critically slow dynamics, and yields a phase boundary narrowing prediction of $\epsilon_c \sim 1/\sqrt{T}$. Indeed, Fig. 2(a)

shows that this scaling fits the experimental data extremely well. In contrast, for the $\mathbb{Z}_2$ and $\mathbb{Z}_3$ cases, signatures of stable DTC order remain but are more fragile, existing only in a relatively narrow region. Furthermore, the scaling of the experimentally obtained phase boundaries differs from the $\mathbb{Z}_2$-Ising case.

The observed universal quadratic scaling of decay rates at sufficiently long T can be qualitatively explained by dephasing of individual spins due to a proliferation of resonances, independent of the details of the thermalizing Hamiltonian. We consider a model [52] where each spin is projected onto its quantization axis within one Floquet cycle due to strong dephasing, leading to Markovian population dynamics, wherein the net ensemble polarization reduces by a factor of $\cos(\epsilon)$ per cycle. This yields a decay rate $\Gamma = -\log[\cos(\epsilon)] \approx \epsilon^2/2$, which agrees well with the experimental observations [Fig. 4(b)] upon allowing for an offset Γ_0 due to external depolarization processes. To probe the origin of dephasing, we perform an additional $\mathbb{Z}_3$ experiment with doubled spin density [52], and find that T^* is halved to $0.21(4)\ \mu$s [Fig. 4(a)]. Moreover, the independently estimated dephasing time due to the external bath is much longer than the T^* values [52], strongly suggesting that dephasing dominantly arises from intrinsic, coherent spin-spin interactions. Indeed, exact diagonalization studies of a strongly interacting toy model of N spin-1/2 particles, coupled via all-to-all random interactions $\sum_{ij} J_{ij}/\sqrt{N}[\alpha(S_i^x S_j^x + S_i^y S_j^y) - S_i^z S_j^z]$ with $\alpha = 0, 1$, and which are periodically rotated by an angle $\pi + \epsilon$, yield a decay rate $\epsilon^2/2$ of the subharmonic signal for sufficiently long Floquet periods $J_{ij}T \gg 1$ [Fig. 4(b)]. However, we note that the Ising case ($\alpha = 0$) shows a much slower approach to the Markovian regime in finite-size scaling than the spin-exchange case ($\alpha = 1$) [52].

Our observations of the relative stability and distinct scaling of the critical DTC regime in the $\mathbb{Z}_2$-Ising case as well as its long T^* value, indicate important differences in the thermalization dynamics of systems with different types of long-range interactions. This is in broad agreement with recent analytical and numerical studies of thermalization [35,40,55]; however, a detailed and better understanding of these differences is a challenging task which deserves further investigation.

Conclusion.—We have demonstrated that the stability of DTC order can be used to sensitively and quantitatively probe thermalization dynamics of a many-body system. In particular, we have explored how the interplay of disorder, periodic driving, and interactions gives rise to different thermalization regimes. Our results shed light on the mechanisms through which many-body quantum systems approach thermal equilibrium, an important aspect in the quest for full control over quantum matter.

We thank N. Y. Yao, K. X. Wei, and G. Kucsko for insightful discussions and experimental assistance. This work was supported in part by MIT-Harvard Center for Ultracold Atoms, Vannevar Bush Fellowship, Army Research Office Multidisciplinary University Research Initiative, Moore Foundation GBMF-4306, Kwanjeong Educational Foundation, Samsung Fellowship, NSF PHY-1506284, NSF DMR-1308435, Japan Society for the Promotion of Science KAKENHI (No. 26220903), EU (FP7, Horizons 2020, ERC), DFG, SNSF, and BMBF.

*These authors contributed equally to this work
†lukin@physics.harvard.edu

[1] J. M. Deutsch, Phys. Rev. A **43**, 2046 (1991).
[2] M. Srednicki, Phys. Rev. E **50**, 888 (1994).
[3] M. Rigol, V. Dunjko, and M. Olshanii, Nature (London) **452**, 854 (2008).
[4] L. D'Alessio, Y. Kafri, A. Polkovnikov, and M. Rigol, Adv. Phys. **65**, 239 (2016).
[5] F. Borgonovi, F. Izrailev, L. Santos, and V. Zelevinsky, Phys. Rep. **626**, 1 (2016).
[6] G. Casati and B. Chirikov, *Quantum Chaos: Between Order and Disorder* (Cambridge University Press, Cambridge, England, 2006).
[7] T. Langen, S. Erne, R. Geiger, B. Rauer, T. Schweigler, M. Kuhnert, W. Rohringer, I. E. Mazets, T. Gasenzer, and J. Schmiedmayer, Science **348**, 207 (2015).
[8] A. M. Kaufman, M. E. Tai, A. Lukin, M. Rispoli, R. Schittko, P. M. Preiss, and M. Greiner, Science **353**, 794 (2016).
[9] P. W. Anderson, Phys. Rev. **109**, 1492 (1958).
[10] I. V. Gornyi, A. D. Mirlin, and D. G. Polyakov, Phys. Rev. Lett. **95**, 206603 (2005).
[11] D. Basko, I. Aleiner, and B. Altshuler, Ann. Phys. (Amsterdam) **321**, 1126 (2006).
[12] R. Nandkishore and D. A. Huse, Annu. Rev. Condens. Matter Phys. **6**, 15 (2015).
[13] D. A. Abanin, E. Altman, I. Bloch, and M. Serbyn, arXiv:1804.11065.
[14] M. Schreiber, S. S. Hodgman, P. Bordia, H. P. Lüschen, M. H. Fischer, R. Vosk, E. Altman, U. Schneider, and I. Bloch, Science **349**, 842 (2015).
[15] J. Smith, A. Lee, P. Richerme, B. Neyenhuis, P. W. Hess, P. Hauke, M. Heyl, D. A. Huse, and C. Monroe, Nat. Phys. **12**, 907 (2016).
[16] J.-y. Choi, S. Hild, J. Zeiher, P. Schauß, A. Rubio-Abadal, T. Yefsah, V. Khemani, D. A. Huse, I. Bloch, and C. Gross, Science **352**, 1547 (2016).
[17] G. Kucsko, S. Choi, J. Choi, P. C. Maurer, H. Zhou, R. Landig, H. Sumiya, S. Onoda, J. Isoya, F. Jelezko *et al.*, Phys. Rev. Lett. **121**, 023601 (2018).
[18] P. Roushan, C. Neill, J. Tangpanitanon, V. Bastidas, A. Megrant, R. Barends, Y. Chen, Z. Chen, B. Chiaro, A. Dunsworth *et al.*, Science **358**, 1175 (2017).
[19] K. X. Wei, C. Ramanathan, and P. Cappellaro, Phys. Rev. Lett. **120**, 070501 (2018).
[20] V. Khemani, A. Lazarides, R. Moessner, and S. L. Sondhi, Phys. Rev. Lett. **116**, 250401 (2016).
[21] D. V. Else, B. Bauer, and C. Nayak, Phys. Rev. Lett. **117**, 090402 (2016).

[22] N. Y. Yao, A. C. Potter, I.-D. Potirniche, and A. Vishwanath, Phys. Rev. Lett. **118**, 030401 (2017).
[23] C. W. von Keyserlingk, V. Khemani, and S. L. Sondhi, Phys. Rev. B **94**, 085112 (2016).
[24] D. V. Else, B. Bauer, and C. Nayak, Phys. Rev. X **7**, 011026 (2017).
[25] W. W. Ho, S. Choi, M. D. Lukin, and D. A. Abanin, Phys. Rev. Lett. **119**, 010602 (2017).
[26] J. Zhang, P. Hess, A. Kyprianidis, P. Becker, A. Lee, J. Smith, G. Pagano, I.-D. Potirniche, A. C. Potter, A. Vishwanath *et al.*, Nature (London) **543**, 217 (2017).
[27] S. Choi, J. Choi, R. Landig, G. Kucsko, H. Zhou, J. Isoya, F. Jelezko, S. Onoda, H. Sumiya, V. Khemani *et al.*, Nature (London) **543**, 221 (2017).
[28] J. Rovny, R. L. Blum, and S. E. Barrett, Phys. Rev. Lett. **120**, 180603 (2018).
[29] S. Pal, N. Nishad, T. S. Mahesh, and G. J. Sreejith, Phys. Rev. Lett. **120**, 180602 (2018).
[30] D. A. Abanin, W. De Roeck, and F. Huveneers, Phys. Rev. Lett. **115**, 256803 (2015).
[31] T. Mori, T. Kuwahara, and K. Saito, Phys. Rev. Lett. **116**, 120401 (2016).
[32] T. Kuwahara, T. Mori, and K. Saito, Ann. Phys. (Amsterdam) **367**, 96 (2016).
[33] D. A. Abanin, W. De Roeck, W. W. Ho, and F. Huveneers, Phys. Rev. B **95**, 014112 (2017).
[34] L. S. Levitov, Phys. Rev. Lett. **64**, 547 (1990).
[35] A. L. Burin, arXiv:cond-mat/0611387.
[36] N. Y. Yao, C. R. Laumann, S. Gopalakrishnan, M. Knap, M. Muller, E. A. Demler, and M. D. Lukin, Phys. Rev. Lett. **113**, 243002 (2014).
[37] A. R. Kolovsky and A. Buchleitner, Europhys. Lett. **68**, 632 (2004).
[38] A. Tomadin, R. Mannella, and S. Wimberger, Phys. Rev. Lett. **98**, 130402 (2007).
[39] L. F. Santos, F. Borgonovi, and F. M. Izrailev, Phys. Rev. Lett. **108**, 094102 (2012).
[40] A. Safavi-Naini, M. Wall, O. Acevedo, A. Rey, and R. Nandkishore, arXiv:1806.03339 [Phys. Rev. A (to be published)].
[41] J. Waugh, L. Huber, and U. Haeberlen, Phys. Rev. Lett. **20**, 180 (1968).
[42] S. Choi, N. Y. Yao, and M. D. Lukin, Phys. Rev. Lett. **119**, 183603 (2017).
[43] A. C. Potter, T. Morimoto, and A. Vishwanath, Phys. Rev. X **6**, 041001 (2016).
[44] C. W. von Keyserlingk and S. L. Sondhi, Phys. Rev. B **93**, 245145 (2016).
[45] C. W. von Keyserlingk and S. L. Sondhi, Phys. Rev. B **93**, 245146 (2016).
[46] R. Roy and F. Harper, Phys. Rev. B **94**, 125105 (2016).
[47] D. V. Else and C. Nayak, Phys. Rev. B **93**, 201103 (2016).
[48] F. Nathan, D. Abanin, E. Berg, N. H. Lindner, and M. S. Rudner, arXiv:1712.02789.
[49] S. Choi, N. Y. Yao, and M. D. Lukin, arXiv:1801.00042.
[50] B. P. Lanyon, C. Hempel, D. Nigg, M. Müller, R. Gerritsma, F. Zähringer, P. Schindler, J. Barreiro, M. Rambach, G. Kirchmair *et al.*, Science **334**, 57 (2011).
[51] M. W. Doherty, N. B. Manson, P. Delaney, F. Jelezko, J. Wrachtrup, and L. C. Hollenberg, Phys. Rep. **528**, 1 (2013).
[52] See Supplemental Material at http://link.aps.org/supplemental/10.1103/PhysRevLett.122.043603 for details about experimental system, theoretical models, data analysis, and numerical simulations.
[53] J. Choi, S. Choi, G. Kucsko, P. C. Maurer, B. J. Shields, H. Sumiya, S. Onoda, J. Isoya, E. Demler, F. Jelezko *et al.*, Phys. Rev. Lett. **118**, 093601 (2017).
[54] L. F. Santos, F. Borgonovi, and G. L. Celardo, Phys. Rev. Lett. **116**, 250402 (2016).
[55] K. S. Tikhonov and A. D. Mirlin, Phys. Rev. B **97**, 214205 (2018).